Chinese Journal of Physiology 52(2): 72-80, 2009
DOI: 10.4077/CJP.2009.AMH015

The Cooperative Phenomenon of Autonomic Nervous System in Urine Storage for Wistar Rats

Shyang Chang[1]*, Meng-Ju Chiang[1, 2], Shiun-Jeng Li[1], Shih-Jen Hu[1], Hsiu-Yao Cheng[3], Sheng-Hwu Hsieh[4], and Chen-Li Cheng[5]*

[1]*Department of Electrical Engineering, National Tsing Hua University*
Hsinchu 300
[2]*Department of Computer and Communication Engineering, Nan Kai Institute of Technology*
Nantou 540
[3]*Department of Chemistry, Tunghai University*
Taichung 407
[4]*Department of Endocrinology and Metabolism, Chang Gung Memorial Hospital,*
Chang Gung University College of Medicine, Taipei 100
and
[5]*Division of Urology, Department of Surgery, Taichung Veterans General Hospital*
Taichung 407, Taiwan, ROC

Abstract

The fractal dimension (FD) and spectral frequencies of physiological signals are two important indices in the study of physiological functions and dynamical diseases. The first index can be used to characterize the *intensity* and the second the *rhythms* of signals embedded in seemingly random data. Recent studies using both indices verified that synergic co-activations of bladder and external urethral sphincter (EUS) of Wistar rats were present during the voiding of urine. In this study, the primary aims were to (1) examine if the involved muscles in the lower urinary tract would be under similar coactivations during the urine storage phase, and (2) characterize quantitatively the sympathetic and parasympathetic nerve activities simultaneously. Eighteen experiments were performed on six intact adult female Wistar rats and then the electromyogram of EUS and cystometrogram of bladder were analyzed. Results indicated that the EUS did not contain any significant spectral frequencies in the storage phase. Furthermore, its FDs (1.5918 ± 0.0157) indicated that no appreciable amount of signal intensities was observed in the EUS. On the other hand, the bladder exhibited parasympathetic frequency of 8 Hz with signal-to-noise ratio (SNR) = 19.9001 decibel (dB) for group mean, and sympathetic frequency of 19 Hz with SNR = 22.8330 dB for group mean. In addition, its FDs (1.4796 ± 0.0092) indicated relatively persistent intensities during storage, as compared to that of EUS (1.5918 ± 0.0157) with statistical significance ($P < 0.01$). We concluded that the EUS was not activated during the phase of storage. The bladder was under the cooperative, not antagonistic, sympathetic and parasympathetic nerve activities with discernible rhythmic frequencies and persistent intensities.

Key Words: autonomic nervous systems, dynamical disease, fractional Brownian motion, micturition, reciprocal innervations, synergic co-activation, urine storage

Corresponding author: Dr. Shyang Chang, Department of Electrical Engineering, National Tsing Hua University, Hsinchu 300, Taiwan 300, ROC. Tel: +886-35731146; Fax: +886-35715971; E-mail: shyang@ee.nthu.edu.tw and Dr. Chen-Li Cheng, Division of Urology, Department of Surgery, Taichung Veterans General Hospital, Taichung 407, Taiwan, ROC. Tel: +886-4-23741215, Fax: +886-4-23593160, E-mail: cheng20011@yahoo.com.tw
*These two authors have equal contribution.
Received: March 26, 2008; Revised (Final Version): September 25, 2008; Accepted: September 30, 2008.
 ISSN : 0304-4920. http://www.cps.org.tw

Introdcution

Ever since Benoit B. Mandelbrot (22) popularized the fractional Brownian motion (FBM) (17) in the 1980s, he and other scientists have applied fractal geometry to various scientific disciplines. The applications range from the most popular research topics, such as human genome project, DNA research, quantum physics, and wavelet analysis to physiological studies (1, 7, 8, 12, 15, 16, 21, 23, 28, 29). Furthermore, by combining fractal dimension (FD) of FBM and power spectral analysis, one can study many systems that exhibit synergic or cooperative phenomena (5, 6, 9, 10). For instance, the lower urinary tract (LUT) includes both the bladder and external urethral sphincter (EUS). The former consists of smooth muscles and is innervated by both sympathetic and parasympathetic nerves, while the latter consists of striated muscles and is innervated by somatic nerves (14, 19, 25). The LUT function contains two phases: the voiding and storage of urine. Most of the time, the LUT is in the urine storage phase and only when the volume of urine in the bladder reaches a threshold and situation permits, will the voiding phase occur. It was believed that during voiding, the EUS had to relax while the bladder was active (2, 3, 4, 18, 19, 20, 26, 27). Thus, the LUT maintained a reciprocal inhibition between the bladder parasympathetic efferent and the ventral somatic efferent of the EUS. Recently, the mechanism of voiding phase in the LUT for female Wistar rats was evaluated (5, 6) *via* FBM and spectral frequencies. The results indicated that the EUS muscle was not relaxed. It was actually contracting in synchronization with the bladder at 7-8 Hz. Moreover, their FDs as functions of time were temporal "coherent" under 1.5 during the voiding phase. These two quantitative indices combined together indicated that the EUS and bladder were synergic rather than antagonistic during the voiding phase.

However, the regulation of LUT during urine storage, another phase that dominated the bladder much of the time was still in dispute. The conventional understanding was that the parasympathetic innervation of the bladder was quiescent while the sympathetic pathway was activated by bladder distension, and the EUS should be contracting as the guarding reflex to provide outlet resistance and urinary continence (3, 4, 11, 26, 27). Thus, the primary aim of this study was to investigate the roles played by the EUS and bladder in urine storage. Furthermore, we would like to quantitatively characterize the autonomic nerve activities *via* the measures of FDs and spectral frequencies.

Materials and Methods

Animal Preparations

To examine the pressure changes of bladder and EUS muscular activities of LUT during urine storage, the female Wistar rats were adopted. A total of 18 micturition experiments were performed on six intact adult female Wistar rats (250–400 g). All experimental procedures were under the guidelines approved by the Institutional Animal Care and Use Committee of Taichung Veterans General Hospital. These Wistar rats were anesthetized with urethane (1.2 g/kg s.c.) before experiments. Normal body temperatures were maintained in the range of 36–38°C by a heating lamp throughout the experimental period. A tracheal cannula was used for artificial ventilation. The arterial blood pressure was monitored *via* a pressure transducer connected to a cannula in the common carotid artery. The bladder was exposed *via* a middle abdominal incision. The rostral half of pubic symphysis was removed to expose the middle urethra and EUS. Two fine insulated silver wire electrodes (0.05 mm diameter) with exposed tips were inserted into lateral sides of midurethra, where muscle fibers of the EUS were identified.

Data Acquisition of Bladder Pressure and EUS Eletromyogram (EMG)

A PE-60 tube was inserted into the apex of the bladder dome through one small incision. To detect intravesical pressure and to infuse physiological saline into the bladder, the PE-60 tube was connected *via* a 3-way stopcock to a pressure transducer and an infusion pump. A cystometrogram (CMG) dataset was obtained by slowly filling the bladder with a rate of 0.123 ml/min. This infusion rate was adjusted to keep the infusion time roughly constant among rats. Each bladder CMG and EUS EMG was recorded continuously *via* a digital acquisition computer-based system (MP100WSW system, BioPac, Goleta, CA, USA) at a sampling rate of 500 points per second. Since the spectral frequencies of Wistar rats' muscles were below 50 Hz, waveforms sampled at 500 points per second could satisfy the sampling theorem. Hence, there was no information loss in data acquisition. A 60-Hz notch filter was also used during data acquisition to reject power line frequency.

Data Analysis

A sliding window method was used both in the calculations of FDs and spectral frequencies. The rationale behind this method was to see how things were changing as one entered different phases by using a combination of time-frequency analysis and temporal fractal structure. For instance, when we slided our observation window from urine storage phase to voiding phase, and vice versa, the dominant

spectral frequencies would emerge and FDs would drop simultaneously for our EMG and differenced CMG. The details of the estimations of FD and spectral frequencies could be found in the literature (5-7, 9, 10). As to the theory of FD, it would be briefly outlined below.

According to Paley and Wiener (24), the Brownian motion $B(t)$ could be defined formally as the integral of an infinite series of oscillations with random amplitudes: $B(t) = \int_0^t \sum_{n=-\infty}^{\infty} \xi_n e^{inx} dx$, where $\{\xi_n\}$ is a sequence of independent, identically distributed standard Gaussian random variables. This integral converges in the L^2 sense and almost surely. It is worth noting that the increments of Brownian motion are stationary and independent (13, 24, 30). However, studies often suggested the existence of strong dependence between samples in applications. Thus, Benoit B. Mandelbrot proposed in 1968 the FBM with correlated stationary increments in real applications (22).

The FBM $\{B_H(t), t \geq 0\}$ with the Hurst parameter H $(0 < H < 1)$ and starting value b_0 at time 0 was defined by $B_H(0) = b_0$, and

$$B_H(t) - B_H(0).$$

$$= \frac{1}{\Gamma(H + 1/2)} \left\{ \int_{-\infty}^{0} [(t-s)^{H-1/2} - (-s)^{H-1/2} dB(s) + \int_0^t (t-s)^{H-1/2} dB(s) \right\}.$$

The increments of this FBM are now dependent but still stationary. The discrete-time fractional Gaussian noise (DFGN) process $\{x_H[n]\}$ is derived from the increment of such sampled FBM. That is, $x_H[n] = B_H[n] - B_H[n-1]$ where $B_H[n] = B_H(nT_s)$ and T_s is the sampling period. The autocorrelation function of a DFGN process, denoted by $r_H[k]$, can be evaluated by the following formula: $E(x_H[n+k]x_H[n]) \equiv r_H[k] = \frac{1}{2}(|k+1|^{2H} - 2|k|^{2H} + |k-1|^{2H})$. Notice that the FBM is clearly reduced to Brownian motion when $H = 1/2$. Hence, the FBM is a generalization of the Brownian motion. The FD is defined as $D = 2 - H$ and would be a scalar value between 1 and 2 since H is between 0 and 1.

The implementation of FBM to our EMG signals was described as follows. For convenience, the width of processing window was set to be 500 points or 1 s. It would be called the "window-size" hereafter. Since the sampling rate was 500 points per second, one data point took 0.002 s and it would be called the "step-size". For EMG, the first window contained the first 500 points of this time series and the first Hurst parameter "*H*" was calculated based on these points. After the first FD was obtained, the window would slide one point to the right along the time axis, the next FD was then calculated. These steps would be carried out repeatedly until the window came to the last 500 points of the time series and the last FD was obtained. Thus, a temporal sequence of FDs for EMG was obtained (6).

As to the CMG, we first took the difference of its time series, and then followed the same computational procedure as that of EMG. We thus obtained a temporal sequence of Hurst parameters for CMG.

The power spectra were computed using a window-size of 500 points so that the resolution of the spectrum was 1 Hz. After the power spectrum of the first window was obtained, the window was then shifted one point to the right and the next power spectrum was calculated. These steps were repeated until the window covered the last 500 points of the time series. All these mathematical computations were performed on an IBM PC desktop (Pentium 4.3 GHz) with Matlab software.

Signal to Noise Ratio (SNR)

Formula SNR = $20 \times \log\left(\frac{signal}{ave\ es}\right)$ was used to calculate the signal to noise ratio of our data. The "*signal*" in the brackets was referred to the value of *es*8, *es*19, *cs*8, or *cs*19 in Tables 1 and 3. Notice that only the numbers 8 and 19 were used here because only 8 Hz and 19 Hz components were observed in our CMG and EMG data. For instance, in Table 1, the notation "*es*8" stood for the normalized unit (n. u.) of *signal* amplitude at 8 Hz in *EMG* during storage phase, and similarly "*cs*19" the *signal* amplitude of 19 Hz component in *CMG*. The "*avg es*" denoted the average amplitude in n. u. of the EMG signals during one experiment. It was used in the computation of SNR, a term that was borrowed from the discipline of communication.

Statistical Analysis

The data for group mean was expressed as means ± SEM. Statistical analyses were performed using the two-tailed Student's *t*-test for unpaired data by Microsoft Excel software. Statistical significance was set at a typical level of $P < 0.01$.

Results

FDs and Spectra of One Complete Storage and Micturition Cycle

To explore the roles of the bladder and EUS, one complete cycle of urine storage and voiding phase was exemplified first. The EMG, CMG, associated

Table 1. Amplitudes of 8 and 19 Hz components in normalized unit (n. u.) during storage phase in one exemplary cycle. Data of 8-second are taken and divided equally into 32 segments, each of 0.25-second. Here, "*es*8" stands for the amplitude in n. u. of 8 Hz component in EMG during one segment of storage phase, and "*cs*19" stands for that of 19 Hz component in CMG during the same segment

Segment	*es*8	*es*19	*cs*8	*cs*19
seg. 1	0.001528	0.001052	0.013659	0.022985
seg. 2	0.001282	0.001294	0.013901	0.020334
seg. 3	0.001853	0.001304	0.013532	0.017291
seg. 4	0.001986	0.001315	0.012248	0.019079
seg. 5	0.001307	0.001224	0.011641	0.022479
seg. 6	0.001150	0.001180	0.013287	0.021785
seg. 7	0.000992	0.001269	0.013223	0.024566
seg. 8	0.001909	0.001292	0.013104	0.022861
seg. 9	0.001736	0.001318	0.011584	0.020561
seg. 10	0.001008	0.001475	0.011143	0.021061
seg. 11	0.000872	0.001114	0.011257	0.023081
seg. 12	0.000937	0.000994	0.011255	0.025675
seg. 13	0.000903	0.000905	0.011217	0.024658
seg. 14	0.000750	0.001003	0.011319	0.018858
seg. 15	0.000962	0.000984	0.011516	0.015615
seg. 16	0.000829	0.000951	0.011309	0.015455
seg. 17	0.000820	0.000860	0.011123	0.014196
seg. 18	0.000952	0.000868	0.012008	0.013022
seg. 19	0.000902	0.000776	0.012335	0.013984
seg. 20	0.000990	0.000942	0.011279	0.013920
seg. 21	0.000730	0.000858	0.010240	0.014026
seg. 22	0.000682	0.000752	0.009444	0.013140
seg. 23	0.000662	0.000876	0.010704	0.007672
seg. 24	0.000732	0.000888	0.012218	0.005205
seg. 25	0.000742	0.001369	0.013064	0.004687
seg. 26	0.000845	0.001311	0.013643	0.005503
seg. 27	0.000968	0.001079	0.013745	0.011444
seg. 28	0.001124	0.001138	0.013202	0.020801
seg. 29	0.001183	0.001594	0.013223	0.024615
seg. 30	0.001314	0.001240	0.013370	0.029133
seg. 31	0.001363	0.001204	0.013141	0.032706
seg. 32	0.001225	0.001149	0.012455	0.033876

FDs and spectral frequencies for the cycle were illustrated in Fig. 1 and Fig. 2, respectively. The temporal FDs of EMG in Fig. 1a exhibited dark blue patterns during voiding within the range of 20 to 25 s. The temporal FDs of CMG in Fig. 1b exhibited the same dark blue patterns during voiding phase within the range of 20 to 22.5 s. The urine storage phase was indicated by the time interval from 0 to 20 s. During this phase, it was clear from Fig. 1 that the EMG and CMG did not have the same color code. As a matter of fact, the FDs of EMG were greater than 1.5 in Fig. 1a, and those of CMG were smaller than 1.5, and they were depicted in the light blue color code in Fig. 1b.

The power spectra of EMG and CMG in Fig. 1 were calculated and displayed in Fig. 2. In this exemplary cycle, there were significant frequencies for EMG at 8 Hz only during voiding phase as in Fig. 2a. However, there was *no* significant frequency component during the storage phase. As to CMG, there were significant frequencies at 8 Hz and 19 Hz throughout the storage phase (Fig. 2b).

To further investigate the amplitudes of 8 Hz and 19 Hz components in bladder and EUS during storage phase, a time span of 8 s on the EMG and CMG data records in Fig. 2 were adopted for comparison (Fig. 3). The 8-second data records were actually divided into 32 segments each with 0.25 s long. Hence, each segment had 125 points according to our sampling rate. The amplitudes of 8 Hz and 19 Hz from both EMG and CMG were presented in n. u. for comparison in Table 1. In Fig. 3, the normalized values of *cs*19 were represented by blue rectangles, and those of *es*19 by red circles. Two green lines x = 0.5 and y = 0.5 were drawn to indicate the contributions from each frequency component. In Fig. 3, the amplitudes of EMG in red circles were much less than 0.1. The SNRs of EMG were computed for comparison. The SNRs at the 8 Hz and 19 Hz components were -2.0850 dB and -2.0020 dB, respectively. Yet, the resultant SNRs of CMG at 8 Hz and 19 Hz were 18.8040 dB and 22.4540 dB. Hence, the SNRs of CMG were much more positive than those of the EMG.

FDs and Spectra of 18 Cycles

Next, we examined the FDs of all 18 urination cycles of six rats. The information of averaged FDs for both voiding and storage phases were presented. Two green lines x = 1.5 and y = 1.5 were drawn to separate the red circles of voiding phase from the blue rectangles of storage phase in Fig. 4. Results indicated that these circles could be separated into two clusters. In this figure, red circles in lower left corner denoted the average FDs of CMG and EMG during voiding phase. Blue rectangles in the middle denoted the average FDs of CMG and EMG during the storage phase. In Table 2, the average value of FDs for CMG was 1.4796 ± 0.0092; and that for EMG was 1.5918 ± 0.0157 (group mean ± SEM for 18 experiments).

Finally, the relative weights of spectral frequencies (19 Hz and 8 Hz) of all 18 urination cycles of six rats were obtained in Fig. 5. An 8-second duration of storage phase was taken for analysis. Thus, there were 18 blue CMG rectangles and 18 red EMG circles. The generating procedure of Fig. 5 was similar to that of Fig. 3 and as before, two green lines x = 0.3 and y =

Table 2. The mean values of FDs for EMG during voiding phase, CMG during voiding phase, EMG during storage phase, and CMG during storage phase in 18 experiments. Group means ± SEM for 18 experiments is listed in the last line

Experiment	FD of EMG during voiding	FD of CMG during voiding	FD of EMG during storage	FD of CMG during storage
exp. 1	1.1453	1.2396	1.5660	1.4235
exp. 2	1.1444	1.2928	1.5689	1.5209
exp. 3	1.1454	1.2275	1.5827	1.4368
exp. 4	1.1535	1.1803	1.5480	1.4889
exp. 5	1.1492	1.1555	1.5534	1.4080
exp. 6	1.1612	1.1661	1.5687	1.4597
exp. 7	1.3379	1.1101	1.6354	1.5005
exp. 8	1.2127	1.0730	1.6866	1.4581
exp. 9	1.1635	1.0836	1.6826	1.4495
exp. 10	1.2670	1.1105	1.6447	1.5232
exp. 11	1.1648	1.0687	1.6548	1.4483
exp. 12	1.2172	1.0844	1.6767	1.5051
exp. 13	1.2186	1.0940	1.6681	1.5602
exp. 14	1.1410	1.1147	1.5001	1.4883
exp. 15	1.1435	1.0671	1.4810	1.4994
exp. 16	1.1476	1.0827	1.4984	1.5160
exp. 17	1.1584	1.0800	1.5838	1.4683
exp. 18	1.1028	1.0836	1.5527	1.4775
means ± SEM	1.1760 ± 0.0131	1.1290 ± 0.0158	1.5918 ± 0.0157	1.4796 ± 0.0092

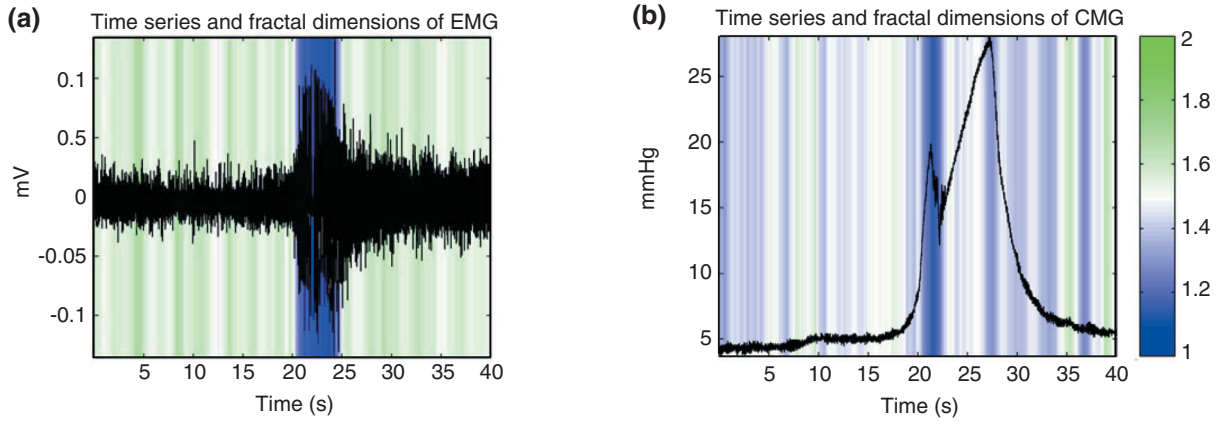

Fig. 1. The EMG, CMG and associated FDs of one complete cycle. Time series of EMG and CMG are represented by black curves and their corresponding FDs are coded in color stripe with the color map in the lower right corner. The green color code is used to denote the values of *D* between 1.5 and 2.0, and blue color code for *D* between 1.0 and 1.5. (a) EMG of EUS and its time course of FDs. (b) CMG and its time course of FDs.

0.2 were drawn to distinguish the red circles of EMG from blue rectangles of CMG. The amplitudes of EMG denoted by red circles in the lower left corner were smaller than those of the CMG (Fig. 5). The SNRs at the 8 Hz and 19 Hz components for CMG *vs.* EMG were 19.9001 ± 1.2240 dB and 22.8330 ± 1.9570 dB *vs.* 0.2240 ± 0.8310 dB and 0.3750 ± 0.7360 dB, respectively (group means ± SEM for 18 experiments) (Table 3).

Discussion

The primary new finding in this study was that the EUS was not activated in the urine storage, and that it was the sympathetic and parasympathetic nerves of the bladder that are coactivated. This finding can

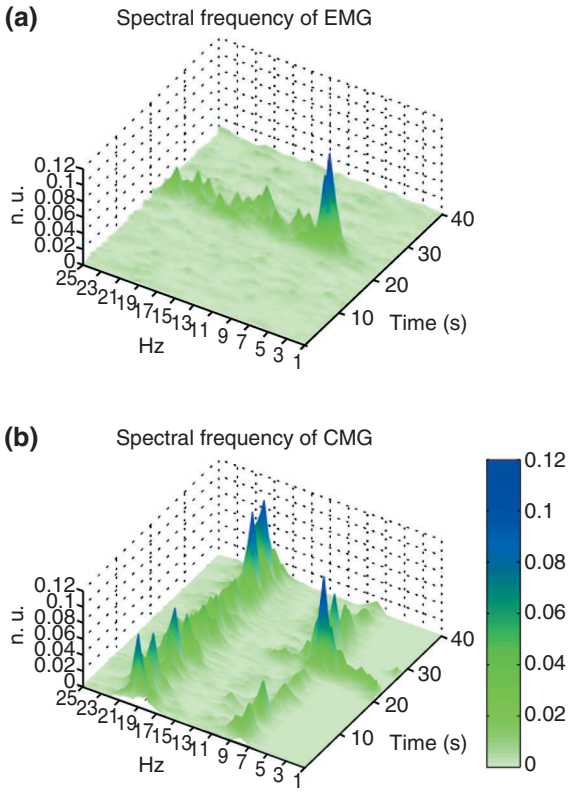

Fig. 2. A 3-D mesh plot of spectral frequencies for one complete cycle including storage and voiding phases. (a) Time-frequency analysis for EMG of EUS. (b) Time-frequency analysis for CMG. The voiding phase is around the neighborhood of 20 seconds. The amplitude of color code is in the lower right corner. The normalized unit of z-axis is denoted by "n. u.". Fig. (a) and (b) are on the same scale and the maximal amplitude 0.12 n.u. is coded in deep blue color.

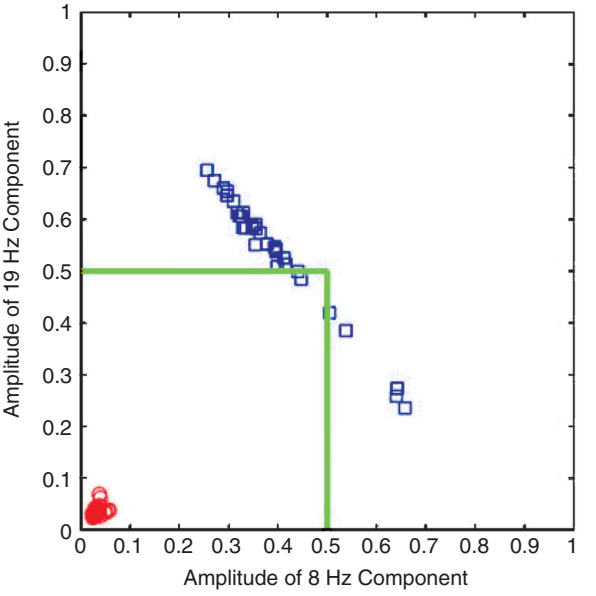

Fig. 3. The 8 Hz and 19 Hz components for CMG (marked by blue "□") and EMG (marked by red "O") during the storage phase of Fig. 2. Two green lines, x = 0.5 and y = 0.5 are drawn to indicate the CMG dominance of 8 Hz and 19 Hz during storage phase.

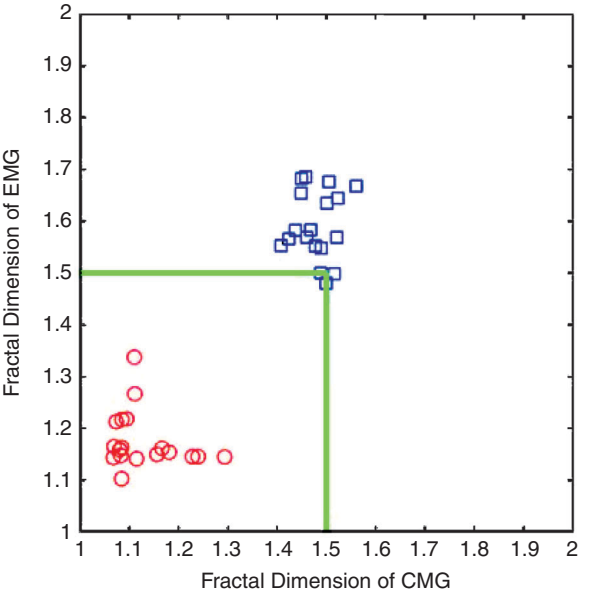

Fig. 4. The FDs of EMG and CMG for 18 complete cycles of urine storage and voiding phases. The 18 red "O" denote FDs during voiding phase while 18 blue "□" denote FDs during storage phase. The red "O" and blue "□" are separated by two green lines, x = 0.5 and y = 0.5.

be initially exemplified from Figs. 1 and 2. Firstly, the FDs of EMG for EUS (Fig. 1a) that exhibited the green patterns during storage corresponded to the average value of 1.5660. It is well-known that if the value is smaller than 1.5, then the muscles will be positively correlated with persistent signal intensity. Hence, the green color code of the storage phase which indicated the muscle fibers of EUS were not positively correlated with persistent intensities. Moreover, there was no significant frequency component during the storage phase (Fig. 2a). Combining both results of FDs and spectral frequencies, we can claim that the EUS was not activated during storage phase for this exemplary cycle.

As to the bladder, the situation was different. The FDs of CMG (Fig. 1b) exhibit light blue color with average FD of 1.4235 for storage phase. It means that the bladder muscles were positively correlated, even though it was not as strong as that in the voiding phase. In addition, there were two groups of significant frequencies at 8 Hz and 19 Hz throughout the storage phase (Fig. 2b). The resultant SNRs of CMG are also much higher than those of the EMG. Hence, combining the results of FD and spectral frequencies, we can claim that the bladder was activated during the storage phase for this exemplary cycle.

Table 3. Average amplitudes of 8 and 19 Hz components in normalized unit (n. u.) during storage phase for 18 experiments. Here, "*es*8" stands for the amplitude in n. u. of 8 Hz component in EMG during storage phase of one experiment, and "*cs*19" stands for that of 19 Hz component in CMG during the same experiment. The "*avg es*" is the average EMG amplitude in n. u. from 1 to 20 Hz during the experiment

Experiment	*es*8	*es*19	*cs*8	*cs*19	*avg es*
exp. 1	0.0022	0.0018	0.0306	0.0320	0.0015
exp. 2	0.0011	0.0011	0.0122	0.0186	0.0014
exp. 3	0.0017	0.0010	0.0249	0.0469	0.0015
exp. 4	0.0023	0.0027	0.0216	0.0227	0.0018
exp. 5	0.0023	0.0017	0.0434	0.0348	0.0015
exp. 6	0.0008	0.0014	0.0170	0.0267	0.0015
exp. 7	0.0025	0.0014	0.0102	0.0479	0.0014
exp. 8	0.0014	0.0015	0.0078	0.0546	0.0013
exp. 9	0.0014	0.0031	0.0161	0.0520	0.0016
exp. 10	0.0014	0.0020	0.0180	0.0204	0.0015
exp. 11	0.0013	0.0023	0.0072	0.0581	0.0017
exp. 12	0.0008	0.0016	0.0176	0.0414	0.0015
exp. 13	0.0011	0.0016	0.0083	0.0244	0.0013
exp. 14	0.0030	0.0018	0.0343	0.0054	0.0027
exp. 15	0.0016	0.0053	0.0116	0.0160	0.0029
exp. 16	0.0054	0.0016	0.0100	0.0062	0.0031
exp. 17	0.0020	0.0013	0.0395	0.0144	0.0019
exp. 18	0.0044	0.0022	0.0282	0.0094	0.0023

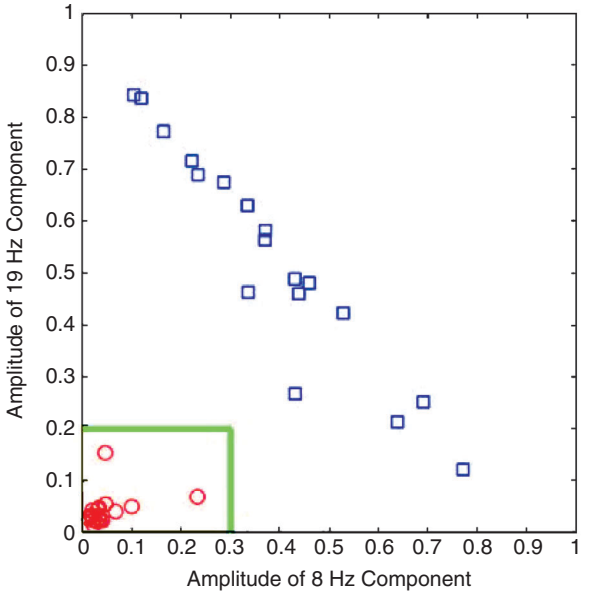

Fig. 5. The 8 Hz and 19 Hz components for CMG (marked by blue "□") and EMG (marked by red "O") during the storage phase of 18 experiments. The blue "□" and red "O" are separated by two green lines, x = 0.3 and y = 0.2.

To characterize quantitatively the sympathetic and parasympathetic nerve activities of urine storage, the frequency components derived from the sympathetic nerve activities will be used. They are usually two to three times faster than the parasympathetic ones (20). Hence, the 8 Hz component is derived from the parasympathetic nerve activities, and the 19 Hz is from the sympathetic nerve activities during the storage phase. In Fig. 3, the 32 blue rectangles were constellating diagonally. The distribution of blue rectangles revealed that the 8 Hz component had 5 rectangles with magnitudes larger than 0.5, and the 19 Hz component had 25 with magnitudes larger than 0.5. This number difference indicated that the sympathetic components of 19 Hz were activated more often than the parasympathetic nerve activities of 8 Hz during this storage phase. Moreover, the normalized amplitudes of 8 Hz and 19 Hz of CMG were greater than 0.2 and far away from 0. Notice that the blue rectangles are distributed rather evenly along the middle of diagonal line (Fig. 3). If these spectral amplitudes were conformable to the antagonistic or reciprocal inhibition model for bladder, the blue rectangles would have clustered near either edge of the diagonal to indicate the excitatory activity by one branch of the autonomic nervous system and the inhibitory activity by the other. However, the blue rectangles in Fig. 3 do not have such kind of distribution. Hence, the behavior of sympathetic and parasympathetic nerve activities is not antagonistic in this exemplary cycle.

Next, all the 18 experiments were examined to see for similarities. For FDs in Fig. 4, their averaged values during voiding and storage phases could be

easily divided into two groups as shown by the green lines. Since the bladder and EUS exhibit synergy during voiding in intact rats, the FDs of CMG and EMG are both under 1.5. Therefore, the red circles representing voiding phase all lie in lower left corner. As to our interest in the storage phase, the FDs for CMG and EMG in Table 2 and Fig. 4 reveal noteworthy difference with $P < 0.01$. The FDs for CMG indicate that there exists positive correlation and persistent intensities among bladder muscles, while the FDs for EUS reflect that the muscle fibers are not positively correlated.

As to the spectral frequencies of all the 18 experiments, the red circles of EMG in the lower left corner of Fig. 5 stand for the fact that the amplitudes of 8 Hz and 19 Hz are insignificantly small, as compared to those of the CMG. The blue rectangles of CMG are also distributed evenly along the middle of diagonal line and not clustered around either one of the edges. Combining the results of FDs and spectral frequencies, we claim that the sympathetic and parasympathetic nerve activities of bladder are both coactivated in a cooperative way. Note that we have used the phrase "synergic coactivation" to indicate the state of *different* muscles having the *same* frequencies and FDs (< 1.5) with persistent intensities (5, 6, 9, 10). Here, the term "cooperative coactivation" is meant to describe the state of the *same* bladder being activated by two *different* nervous systems with discernible frequencies and FDs (< 1.5) indicating persistent intensities. The sympathetic firing is perhaps activated for the purpose of vasodilatation that is required to adjust the bladder compliance for filling and prevent it from being overactive. The parasympathetic firing is perhaps necessary to maintain the responsiveness of bladder and prevent it from being flaccid and underactive. It is worth mentioning that the urinary bladder of human beings is different from that of rats. From the developmental point of view, the human beings are meant to stand straight up while rats crawl in prone position. Hence, the human bladder outlet is developed in the vertical downward position while bladder outlet of rats is in horizontal. Thus, the EUS structure and function in human beings can be much more complex than those of the rats. Consequently, the results obtained in this study are applicable only to the bladders of female rats. As to human beings, it will be worth studying in the future.

In conclusion, by combining FDs and spectral frequencies, we are able to characterize both the sympathetic and parasympathetic nerve activities of the bladder. It is fitting to say that during urine storage the EUS is not activated; it is the bladder that plays an important role. The sympathetic and parasympathetic nerve activities of the bladder are found to be cooperative rather than antagonistic in female Wistar rats by invoking FDs and spectral frequencies. The obtained results will definitely be helpful to us in understanding the dynamical disease of LUT. Finally, we believe that the studies of this paper and related works (5-10) can be beneficial for us in reevaluation of the concept of reciprocal inhibition.

Acknowledgments

We would like to thank Ms. Wen-Ching Lin of Taichung Veterans General Hospital for having conducted the animal experiments and provided the data for this paper.

This work was supported in part under the Grant number NSC 97-2221-E-007-072 of NSC.

References

1. Arneodo, A., d'Aubenton-Carafa, Y., Bacry, E., Graves, P.V., Muzy, J.F. and Thermes, C. Wavelet based fractal analysis of DNA sequences. *Physica D* 96: 291-320, 1996.
2. Barrington, F.J.F. The component reflexes of micturition in the cat. *Brain* 54: 177-188, 1931.
3. Chancellor, M.B. and Yoshimura, N. Physiology and pharmacology of the bladder and urethra. In: Campbell's Urology, 8th ed., edited by Walsh, P.C. Philadelphia, PA: Saunders, 2002, pp. 831-886.
4. Chancellor, M.B. and Yoshimura, N. Neurophysiology of stress urinary incontinence. *Rev. Urol.* 6 (Suppl 3): S19-S28, 2004.
5. Chang, S., Hu, S.J. and Lin, W.C. Fractal dynamics and synchronization of rhythms in urodynamics of female Wistar rats. *J. Neurosci. Meth.* 139: 271-279, 2004.
6. Chang, S., Li, S.J., Chiang, M.J., Hu, S.J. and Hsyu, M.C. Fractal dimension estimation *via* spectral distribution function and its application to physiological signals. *IEEE Trans. Biomed. Eng.* 54: 1895-1898, 2007.
7. Chang, S., Mao, S.T., Hu, S.J., Lin, W.C. and Cheng, C.L. Studies of detrusorsphincter synergia and dyssynergia during micturition in rats *via* fractional Brownian motions. *IEEE Trans. Biomed. Eng.* 47: 1066-1073, 2000.
8. Chang, S., Mao, S.T., Kuo, T.P., Hu, S.J., Lin, W.C. and Cheng, C.L. Fractal geometry in urodynamics of lower urinary tract. *Chinese J. Physiol.* 42: 25-31, 1999.
9. Chang, S., Hsyu, M.C., Cheng, H.Y. and Hsieh, S.H. Synergic coactivation of muscles in elbow flexion *via* fractional Brownian motion. *Chinese J. Physiol.* 51: 376-386, 2008.
10. Chang, S., Hsyu, M.C., Cheng, H.Y., Hsieh, S.H. and Lin, C.C. Synergic coactivation in forearm pronation. *Ann. Biomed. Eng.* PMID: 18802753, Sept. 19, 2008.
11. De Groat, W.C., Downie, J.W., Levin, R.M., Long Lin, A.T., Morrison, J.F.B., Nishizawa, O., Steers, W.D. and Thor, K.D. Basic neurophysiology and neuropharmacology, In: Incontinence, edited by Abrams, P., Khoury, S. and Wein, A. Plymouth, UK: Plymouth Distributors Ltd, 1999, pp. 105-155.
12. Embrechts, P. and Maejima, M. Selfsimilar Processes. Princeton: Princeton University Press, 2002.
13. Feder, J. Fractals. New York and London: Plenum Press, 1988.
14. Gaskell, W.H. The Involuntary Nervous System. London, Longmans: Green and Co. 1916.
15. Hao, B.L., Lee, H.C. and Zhang, S.Y. Fractals related to long DNA sequences and complete genomes. *Chaos, Solitons & Fractals* 11: 825-836, 2000.
16. Karanikas, C. The Hausdorff dimension of very weak self-similar

fractals described by the Haar wavelet system. *Chaos, Solitons & Fractals* 11: 275-280, 2000.
17. Kolmogorov, A.N. Wienersche Spiralen und einige andere interessante Kurven im Hilbertschen Raum, *C.R. (Doklady) Acad. Sci. USSR* 16: 115-118, 1940.
18. Kruse, M.N., Belton, A.L. and de Groat, W.C. Changes in bladder and external urethral sphincter function after spinal cord injury in the rat. *Am. J. Physiol.* 264: 1157-1163, 1993.
19. Langley, J.N. The Autonomic Nervous System. England, Cambridge: Heftier & Sons, 1921.
20. Langworhty, O.R., Kolb, L.C. and Lewis, L.G. Physiology of Micturition. Baltimore: The Williams & Wilkins Company, 1940.
21. Liu, S.C. and Chang, S. Dimension estimation of discrete-time fractional Brownian motion with applications to image texture classification. *IEEE Trans. Image Processing* 6: 1176-1184, 1997.
22. Mandelbrot, B.B. The Fractal Geometry of Nature. San Francisco: Freeman, 1982.
23. Nottale, L. On the transition from the classical to the quantum regime in fractal space-time theory. *Chaos, Solitons & Fractals* 25: 797-803, 2005.
24. Paley, R.E.A.C. and Wiener, N. Fourier Transforms in the Complex Domain. vol. 19. American Mathematical Society Providence, R. I., 1934.
25. Sheehan, D. Discovery of the autonomic nervous system. *Arch. Neurol. Psychiat.* XXXV: 1081-1115, 1936.
26. Shefchyk, S.J. Sacral spinal interneurones and the control of urinary bladder and urethral striated sphincter muscle function. *J. Physiol.* 533: 57-63, 2001.
27. Standring, S. Gray's Anatomy. New York: Churchill Livingstone, 2005.
28. Billock, V.A., de Guzman, G.C. and Scott Kelso, J.A. Fractal time and 1/f spectra in dynamic images and human vision. *Physica D* 148: 136-146, 2001.
29. Voss, R.F. Fractals in nature: From characterization to simulation. In: The Science of Fractal Images, edited by Peitgen, H.O. and Saupe, D. New York: Springer-Verlag, 1988, pp. 21-70.
30. Yaglom, A.M. An Introduction to the Theory of Stationary Random Functions; Rev. English Dover ed. New York: Dover Pub., 1973.